



Acid-Sensing Ion Channels Expression, Identity and Role in the Excitability of the Cochlear Afferent Neurons

Antonia González-Garrido¹, Rosario Vega¹, Francisco Mercado², Iván A. López³ and Enrique Soto^{1*}

¹ Instituto de Fisiología, Benemérita Universidad Autónoma de Puebla, Puebla, Mexico, ² Dirección de Investigaciones en Neurociencias, Instituto Nacional de Psiquiatría Ramón de la Fuente Muñiz, México D.F., Mexico, ³ Department of Head and Neck Surgery, David Geffen School of Medicine, University of California, Los Angeles, CA, USA

OPEN ACCESS

Edited by:

Egidio D'Angelo,
University of Pavia, Italy

Reviewed by:

Jürg Streit,
University of Bern, Switzerland
Robert Weissert,
University of Regensburg, Germany

*Correspondence:

Enrique Soto
esoto24@gmail.com

Received: 10 September 2015

Accepted: 30 November 2015

Published: 22 December 2015

Citation:

González-Garrido A, Vega R, Mercado F, López IA and Soto E (2015) Acid-Sensing Ion Channels Expression, Identity and Role in the Excitability of the Cochlear Afferent Neurons. *Front. Cell. Neurosci.* 9:483. doi: 10.3389/fncel.2015.00483

Acid-sensing ion channels (ASICs) are activated by an increase in the extracellular proton concentration. There are four genes (ASIC1-4) that encode six subunits, and they are involved in diverse neuronal functions, such as mechanosensation, learning and memory, nociception, and modulation of retinal function. In this study, we characterize the ASIC currents of spiral ganglion neurons (SGNs). These ASIC currents are primarily carried by Na⁺, exhibit fast activation and desensitization, display a pH₅₀ of 6.2 and are blocked by amiloride, indicating that these are ASIC currents. The ASIC currents were further characterized using several pharmacological tools. Gadolinium and acetylsalicylic acid reduced these currents, and FMRFamide, zinc (at high concentrations) and *N,N,N',N'*-tetrakis-(2-piridilmetil)-ethylenediamine increased them, indicating that functional ASICs are composed of the subunits ASIC1, ASIC2, and ASIC3. Neomycin and streptomycin reduced the desensitization rate of the ASIC current in SGNs, indicating that ASICs may contribute to the ototoxic action of aminoglycosides. RT-PCR of the spiral ganglion revealed significant expression of all ASIC subunits. By immunohistochemistry the expression of the ASIC1a, ASIC2a, ASIC2b, and ASIC3 subunits was detected in SGNs. Although only a few SGNs exhibited action potential firing in response to an acidic stimulus, protons in the extracellular solution modulated SGN activity during sinusoidal stimulation. Our results show that protons modulate the excitability of SGNs via ASICs.

Keywords: ASIC, inner ear, auditory, Corti, spiral ganglion, aminoglycosides, acetylsalicylic acid, FMRFamide

Abbreviations: ADI, Alpha Diagnostic International; AP, action potential; ASA, acetylsalicylic acid; ASIC, acid-sensing ion channel; B, brain; BSA, bovine serum albumin; cDNA, complementary deoxyribonucleic acid; CNS, central nervous system; DAB, diaminobenzidine; DNA, deoxyribonucleic acid; DRG, dorsal root ganglia; ENaC/DEG, epithelial sodium channels/degenerin; HEPES, 4-(2-hydroxyethyl)-1-piperazineethanesulfonic acid; IHC, inner hair cell; *I*_{int}, integral of the current; *I*_{peak}, peak current; IR, immunoreactivity; *I*_{sub}, sustained current; *K*_{Na}, Na⁺-activated potassium current; MES, 2-(*N*-morpholino) ethanesulfonic acid; Neo, neomycin; OC, organ of Corti; PBS, phosphate buffer solution; PNS, peripheral nervous system; RNA, ribonucleic acid; mRNA, messenger ribonucleic acid; SG, spiral ganglion; SGN, spiral ganglion neuron; St, streptomycin; TPEN, *N,N,N',N'*-tetrakis-(2-piridilmetil)-etilendiamina; τ_{des} , desensitization tau.

INTRODUCTION

Acid-sensing ion channels belong to the ENaC/DEG family. Four *Asic* genes (*Accn1-4*) encode six different subunits: ASIC1a, ASIC1b, ASIC2a, ASIC2b, ASIC3 and ASIC4. These channels are expressed in the CNS and PNS. ASICs participate in synaptic plasticity, learning and memory, and fear conditioning (Wemmie et al., 2002, 2003; Du et al., 2014). In the retina, ASICs participate in synaptic transmission and neuroprotection. ASIC1a plays a significant role in cone function (Ettaiche et al., 2006), and ASIC2 plays a protective role against light-induced degeneration (Ettaiche et al., 2004). ASICs have been found to modulate the synaptic input of vestibular afferent neurons in the rat (Mercado et al., 2006, 2012) and axolotl (Vega et al., 2009).

ASICs participate in the pathophysiology of several CNS diseases. In epilepsy, ASIC1a activation in inhibitory neurons terminates seizure events (Ziemann et al., 2008). During ischemic episodes, blocking ASIC1a significantly reduces the infarct zone, protecting the brain from a major injury type. In the PNS, ASICs have been associated with inflammatory pain (Yagi et al., 2006; Deval et al., 2008). In a murine model of multiple sclerosis, ASIC1 gene deletion or the administration of specific ASIC blockers reduced the progression of neurodegeneration (Friese et al., 2007). Glutamatergic vesicles have a pH of approximately 5.7, and its release causes pH fluctuations in the synaptic cleft (Miesenböck et al., 1998; Du et al., 2014). The pH decrease in the synaptic cleft during synaptic activity is sufficient to activate ASIC, thus modulating postsynaptic membrane excitability (Du et al., 2014).

Glutamate is the primary afferent neurotransmitter in the auditory system. Its release from cochlear hair cells by ribbon synapses provides rapid and continuous input to afferent boutons, resulting in signals that strictly encode the time-course and intensity of sound (Goutman and Glowatzki, 2007). ASIC2 knockout mice exhibit increased resistance to noise-induced temporary threshold shifts (Peng et al., 2004), indicating a function of this subunit in hearing and the potentially harmful effects of acidosis (Sherwood et al., 2011). SGNs and the OC express ASIC3 (Hildebrand et al., 2004). Although ASIC3 knockout mice exhibit normal hearing, they develop hearing loss early in life (4 months of age) (Hildebrand et al., 2004). Additionally, the ASIC1b subunit was detected in SGNs and in the stereocilia bundle of mouse cochlear hair cells (Ugawa et al., 2006). Despite efforts to determine the role of ASIC channels in hearing, its role remains unclear. In this study, we characterize these ion channels in SGNs. Using the patch-clamp technique, we provide physiological and pharmacological evidence indicating the presence of all ASIC subunits in SGNs. RT-PCR and immunohistochemistry analyses revealed that four ASIC subunits are expressed in SGNs. Current-clamp experiments demonstrated that ASICs transmit excitatory input to SGNs, which may significantly modulate their electrical behavior.

MATERIALS AND METHODS

C57/BL mice of either sex were used for the experiments. The animal care and procedures were performed in accordance with the National Institutes of Health Guide for the Care and Use of Laboratory Animals and the *Reglamento de la Ley General de Salud en Materia de Investigación para la Salud* of the *Secretaría de Salud de México*. Protocols involving animal research were reviewed and approved by the Institutional Committee of Use and Care of Laboratory animals (CICUAL) from Research and Postgraduate Vicerectory of the Benemérita Universidad Autónoma de Puebla (VIEP-BUAP). All efforts were made to minimize the suffering and to reduce the number of animals used, as outlined in the “Guide to the Care and Use of Laboratory Animals” issued by the National Academy of Sciences. Animals were supplied by the “Claude Bernard” animal facility of the Universidad Autónoma de Puebla where they were maintained in pathogen-free conditions using isolator for rats provided with disposable HEPA filters.

SGN Cell Culture

Postnatal day 3 to 5 (P3–5) and 14 to 16 (P14–16) mice were used to obtain the SGN primary culture (Valdés-Baizabal et al., 2015). The mice were anesthetized using sevoflurane (Pisa Farmacéutica, Guadalajara, México) and were decapitated. SGNs were isolated and dissect from both inner ears and were incubated (30 min at 37°C) in 1.25 mg/ml trypsin and 1.25 mg/ml collagenase (both from Sigma–Aldrich, St. Louis, MO, USA)- diluted in L-15 medium (Sigma–Aldrich). After enzyme treatment, the ganglia were washed three times with sterile L-15 medium. The cells were mechanically dissociated using a Pasteur pipette and then seeded on 12 mm × 10 mm glass coverslips (Corning, Corning, NY, USA) pretreated with poly-D-lysine (Sigma–Aldrich). These neurons were incubated for 18–24 h in a humidified atmosphere (95% air and 5% CO₂ at 37°C) using a CO₂ water-jacketed incubator (Nuaire, Plymouth, MN, USA). The L-15 medium used for cell culture contained 15.7 mM NaHCO₃ (Merck, Naucalpan, México), 10% fetal bovine serum (Gibco, Grand Island, NY, USA), 100 IU/ml penicillin (Lakeside, Toluca, México) and 15.8 mM HEPES (Sigma–Aldrich).

Voltage- and Current-Clamp Recording

The patch clamp recordings were performed in SGN from P3–5 mice. Further, some recordings were performed in SGN from P14–16 mice were done to identify the ASIC current presence after the onset of hearing stage. To record ionic currents and voltage responses whole-cell patch-clamp technique was used. The cellular responses were examined according to standard voltage- and current-clamp protocols at room temperature (23–25°C) using an Axopatch 1D amplifier (Molecular Devices, Union City, CA, USA). The cells selected for recording were not adherent to other cells, did not display any neurite outgrowth, and exhibited a round, birefringent soma. Command-pulse generation and data sampling were controlled using pClamp

9.0 software (Molecular Devices) and a 16-bit data-acquisition system (Digidata 1320, Molecular Devices). The signals were low-pass filtered at 5 kHz and were digitized at 10 kHz. Patch pipettes were pulled from borosilicate glass capillaries (TW120-3; WPI, Sarasota, FL, USA) using a Flaming–Brown electrode puller (80/PC; Sutter Instruments, San Rafael, CA, USA). The electrodes typically displayed a resistance of 2–3 M Ω when filled with an internal solution of the following composition (mM): 10 NaCl, 125 KCl, 0.1 MgCl₂, 10 EGTA, 1 Na-GTP, 2 Mg-ATP, and 10 HEPES (pH 7.3 adjusted with KOH). The osmolarity of the internal solution was adjusted to 300 mOsm. Approximately 80% of the series resistance was electronically compensated. Throughout the time-course of each experiment, the seal and the series resistance were continuously monitored to confirm stable recording conditions. The recording was not included in the analysis if the access resistance changed >10%.

For the current-clamp recordings, the cell membrane voltage was maintained near –60 mV. The cells were stimulated with sinusoidal current injection (33120A 15 MHz Arbitrary/Waveform Generator; Hewlett-Packard, Palo Alto, CA, USA). The frequency of the stimulus ranged from 10 to 30 Hz, and the stimulus amplitude ranged from 200 to 600 pA. As in the voltage-clamp recordings, the low pH solution was applied for 5 s.

Solutions, Drugs, and Experimental Design

The cells were bath-perfused with extracellular solution containing (mM) 140 NaCl, 5.4 KCl, 2 MgCl₂, 1.8 CaCl₂, 10 glucose, and 10 HEPES. The pH of the extracellular solution was adjusted to 7.4 using NaOH. For those solutions whose pH was <6.5, the buffer MES was used instead of HEPES. The external solutions were adjusted to pH 8, 7.8, 7.6, 7.4, 7.2, 7.0, 6.5, 6.1, 5.5, 5.0, or 4.0. The osmolarity was monitored using a vapor pressure osmometer (Wescor, Logan, UT, USA) and was adjusted to 290 mOsm using dextrose. In some experiments, NaCl was equimolarly substituted with LiCl or Choline-Cl. A gravity-driven perfusion system maintained the external solution flow into the chamber at a rate of approximately 100 μ l/min. To examine the responses of the cells to pH changes or to different drugs used, the recorded cells were perfused using a square-tube fast solution-changer (SF-77B Warner Inst., Hamden, CT, USA) change from one perfusion solution to another was in \sim 20 ms. To examine the currents produced by the acidic solutions, the cells were voltage-clamped at a holding potential of –60 mV (approximately the normal resting potential of SGNs) and were perfused for 5 s with the test solution. In all of the experiments, at least two control responses were recorded before any experimental manipulation to assure that the cells maintain a stable acid-activated current. For perfusion of the drugs, the protocols were performed as described by Garza et al. (2010): (i) preapplication consisted of drug application for 10 s followed by perfusion of the pH 6.1 acid solution for 5 s; (ii) sustained application consisted of drug application for the preceding 10 s and during the 5 s acid solution perfusion; and (iii) coapplication

consisted of drug application only during the 5 s acid solution perfusion.

The drugs used were: FMRFamide, ASA, amiloride, ST sulfate, Neo sulfate, and TPEN. Also, GdCl₃ and ZnCl₂ were used (all from Sigma–Aldrich). These drugs were freshly prepared before the experiments, and 10 μ M capsazepine (Sigma–Aldrich) was added to all of the experiments to avoid the potential activation of TRPV1 channels in SGNs (Mercado et al., 2006).

Data Analysis

For each experimental condition, a control and a washout recording were obtained. The data were analyzed offline using Clampfit 9.2 software (Molecular Devices); the parameters measured in proton-gated currents were the I_{peak} amplitude (I_{peak}) and the I_{sus} amplitude, measured as the mean of the current during the final 250 ms of the 5 s acid pulse. The current desensitization was fitted with a single exponential function obtaining a desensitization time constant (τ_{des}). To construct the current versus pH curve, the I_{peak} values were normalized to that at pH 4. The pH-response curve was fitted with the function

$$Y = \min + (\max - \min)/(1 + (x/EC_{50})^H),$$

where x is the pH, max and min are the maximum and the minimum I_{peak} , EC_{50} is the concentration at which 50% of the I_{peak} is detected, and H is the Hill slope constant. To evaluate the statistical significance of the data, a paired Student's t -test or one-way ANOVA was used, and $P < 0.05$ was considered to be significant. The experimental data are presented as the mean \pm standard error of the mean (SEM).

Immunohistochemistry

C57/BL mice from postnatal day 25 (P25) were euthanized via an overdose of sevoflurane (Pisa Farmacéutica) and were perfused with 4% paraformaldehyde (pH 7.2) in 0.1 M sodium phosphate buffer. The temporal bones were removed from the skull, immersed in the same fixative for 4 h, and decalcified via immersion in a 5% EDTA phosphate-buffered solution for 5 days. The auditory bullae were further immersed in 30% sucrose. Midmodiolar sections (20 μ m thick) were made using a cryostat (Microm HM 500, Zeiss, Oberkochen, Germany). The sections were mounted on glass slides (Superfrost-plus, Fisher Scientific, Leicestershire, England) and stored at –80°C until further use. For the study of ASIC expression in neurons after 24 h in culture the cells were fixed with 4% paraformaldehyde for 30 min and were washed in PBS.

For immunofluorescence, the tissue sections and cultured cells were incubated at room temperature for 30 min in a blocking solution containing 5% normal goat serum, 5% normal horse serum, and 0.5% BSA (fraction V, Sigma) in 0.1% Triton X100 in PBS. Next, tissue sections and cultured neurons were exposed to the primary polyclonal antibody against pan-ASIC1, pan-ASIC2, ASIC3, or ASIC4 diluted 1:200 (Abcam, Cambridge, MA, USA). To further corroborate ASIC expression in SGNs, a second experimental series (ADI series) of tissue sections were exposed to a different set of primary antibodies against ASIC1a, ASIC1b, ASIC2a, ASIC2b, ASIC3, or ASIC4 diluted 1:500 (ADI,

San Antonio, TX, USA). All of these incubations were performed in a humidified chamber at 4°C for 48 h. After this incubation, the samples were washed three times for 10 min in PBS. Then, the samples were incubated in an Alexa Fluor 488-conjugated secondary antibody (1:1,000; Molecular Probes, Eugene, OR, USA) for 1 h at room temperature in the dark. The tissue sections were washed with PBS and then mounted using Vectashield solution (Vector Labs, Burlingame, CA, USA).

For immunoperoxidase staining, the sections were incubated for 1 h in a blocking solution containing 3% normal goat serum in 1% BSA (Sigma–Aldrich) and 0.5% Triton X-100 (Sigma–Aldrich) in PBS. Incubation in primary antibodies against ASIC subunits was done for 16 h at 4°C. The sections were washed with PBS (3 × 10 min) and incubated in biotinylated secondary antibody for 1 h (goat anti-rabbit IgG, 1:500) (Vector Labs), followed by incubation in Vectastain Elite ABC reagent (Vector Labs) for 1 h. Immunoperoxidase staining was performed using DAB reagent kit (Vector Labs). The slides were mounted using Permount mounting media (Fisher Scientific).

Negative controls were generated by incubating a pre-absorbed primary antibody in the corresponding blocking peptide (ADI) or by omitting the ASIC antibodies during the immunohistochemical procedure. The mouse DRG were used as positive controls for all subunits, and the cerebellar cortex was used as a positive control for ASIC2a. The tissue slices and cultured cells were observed using an Olympus FV1000 confocal microscope (Olympus, Tokyo, Japan). The ADI series of immunostained tissue sections was observed and imaged using an Eclipse E800 microscope (Nikon, Tokyo, Japan) equipped with an RTslider spot digital camera (Diagnostics Instruments, Sterling Heights, MI, USA) and ImagePro Plus software (Media Cybernetics, Silver Spring, MD, USA). All histological figures were prepared using Adobe Photoshop software (Adobe Systems Incorporated, San Jose, CA, USA).

RT-PCR

Spiral ganglion (SG) and Brain were dissected from P3-5 C57/BL mice and RNA was isolated using the TRIzol reagent method (Invitrogen). The RT-PCR experiments were done three times ($n = 3$); for each experiment, tissue from the inner ear of eight mice was pooled. The tissues were homogenized with a pellet pestle (Sigma–Aldrich) in TRIzol reagent, and total RNA was obtained according to the manufacturer's instructions. The extracted RNA was treated with DNase I (Invitrogen) to eliminate the genomic DNA. The RNA quantity ($>10 \mu\text{g}/\mu\text{l}$) and purity ($A_{260}/A_{280} > 1.6$) were verified by spectrophotometry, and the RNA integrity was confirmed via 2% agarose gel electrophoresis. cDNA was synthesized using the SuperScript First-Strand Synthesis Supermix kit (Invitrogen). PCR was done in a 25 μl reaction volume using cDNA as template. Primers to amplify the *Asic1*, *Asic2*, *Asic3*, and *Asic4* mRNA were purchased from SABioscience–Qiagen, (Venlo, Netherlands; cat No. PPM32346A-200, PPM04118E-200, PPM38994A-200, PPM30788A-200, respectively). The 18S ribosomal primer (PPM57735E-200) was used as the constitutive-expression control. The predicted band size for each primer pair was 99, 169, 142, 116, and 129 for *Asic1-4* and 18S, respectively. For PCR of

negative controls, the RT procedure was omitted. Amplification was conducted using a Mini-Opticon thermal cycler (Bio-Rad, Hercules, CA, USA). The PCR products were labeled with ethidium bromide in a 2% agarose gel, and the image was taken in an UV transilluminator.

RESULTS

ASIC Current Characteristics

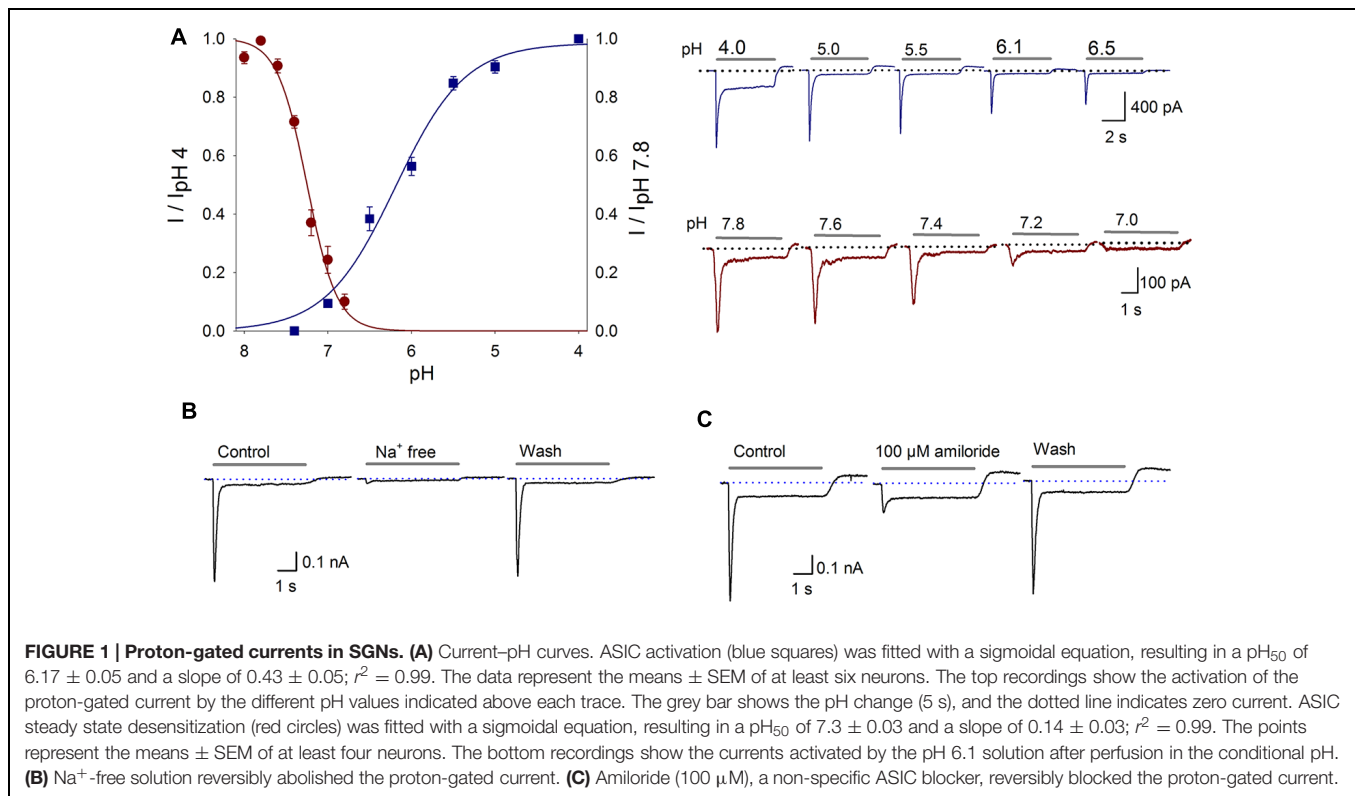
To determine the pH dependency of the proton-gated current of the SGN, the current was activated with extracellular solutions of different pH values: 4.0, 5.0, 5.5, 6.1, 6.5, or 7.0; the current-pH curve displayed a pH_{50} of 6.17 ± 0.05 and a slope of 0.43 ± 0.05 (Figure 1A, $n \geq 6$). Therefore, in subsequent experiments, a pH 6.1 extracellular solution was used to activate the ASIC current. To further characterize the proton-gated current, the steady-state desensitization was determined. SGNs were perfused for 1 min with different pH extracellular solutions (8.0, 7.8, 7.6, 7.4, 7.2, 7.0, 6.8, or 6.6), and then current was activated using a pH 6.1 solution, the fitted current-pH curve displayed a pH_{50} of 7.3 ± 0.03 and a slope of 0.14 ± 0.03 (Figure 1A, $n \geq 4$).

To determine if Na^+ is the predominant permeant ion, a Na^+ -free extracellular solution was used (NaCl was equimolarly replaced with choline-Cl, pH 7.4 or 6.1). The I_{peak} of the proton gated current was reduced in 92% respect to control value with a Na^+ -free solution ($P < 0.05$, $n = 10$), indicating that the proton-gated current is essentially carried by Na^+ influx (Figure 1B).

Pharmacological Characterization of the ASIC Current

To further characterize this proton-gated current in SGNs, amiloride (a nonspecific ASIC blocker) was used. Amiloride (100 μM) reduced the acid-gated I_{peak} by $72 \pm 2\%$ ($P < 0.05$, $n = 6$) and increased the τ_{des} by $40 \pm 9\%$ ($P < 0.05$), although no significant change in the I_{sus} was detected (Figure 1C). The sensitivity of the proton-gated current in SGNs to amiloride and the finding that this current was attributed to Na^+ indicate that it is an ASIC-mediated current.

Application of 100 μM Gd^{3+} reduced the I_{peak} by $67 \pm 9\%$ ($P < 0.05$, $n = 6$), although no change in the I_{sus} or the τ_{des} was detected (Figure 2A). It has been reported that high concentrations (high μM range) of Zn^{2+} increase the current in ASIC heteromers, including those containing the ASIC2a subunit (Baron et al., 2001), and that low concentrations (low nM range) of Zn^{2+} constitutively block the ASIC1a subunit (Chu et al., 2004). In our experiments, the coapplication of 300 μM Zn^{2+} to SGNs increased the current amplitude by $62 \pm 11\%$ ($P < 0.05$, $n = 6$), although no significant change in the I_{sus} or the τ_{des} was detected, indicating that the ASIC2a subunit is functionally expressed in the ASIC heteromers in SGNs (Figure 2B). By contrast, sustained perfusion of 100 μM Zn^{2+} increased the I_{peak} by $35 \pm 11\%$ ($P < 0.05$, $n = 6$) but did not affect the I_{sus} or the τ_{des} (Figure 2C). Additionally, sustained 300 μM Zn^{2+} application increased the τ_{des} by $138 \pm 29\%$ ($P < 0.01$, $n = 5$) but did not affect the I_{peak} or the I_{sus} (Figure 2D).



The sustained application of $10 \mu M$ TPEN (a high-affinity Zn^{2+} chelator) enhanced the ASIC current by $31 \pm 12\%$ ($P < 0.05$, $n = 5$) but did not alter the I_{sus} or the τ_{des} (Figure 2E), indicating that ASIC1a is functionally expressed in SGNs. The application of $300 \mu M$ ASA reduced the amplitude of the proton-gated current by $27 \pm 5\%$ ($P < 0.01$, $n = 9$) and increased the τ_{des} by $20 \pm 7\%$ ($P < 0.05$), but no significant change in the I_{sus} was detected (Figure 2F). Because ASA and Gd^{3+} modulate ASIC3 containing channels, these results indicate that ASIC3 is functionally expressed in SGNs.

FMRamide-like peptides potentiate ASIC1- and ASIC3-containing channels (Askwith et al., 2000). In our experiments, pre-application of $100 \mu M$ FMRamide increased the τ_{des} by $89 \pm 22\%$ ($P < 0.05$, $n = 10$) and the I_{sus} by $40 \pm 12\%$ ($P < 0.05$) but did not significantly affect the I_{peak} (Figure 2G).

The set of pharmacological tools used indicate that proton-gated currents in SGNs are mediated by ASIC channels composed of at least ASIC1, ASIC2, and ASIC3 (Figure 2H).

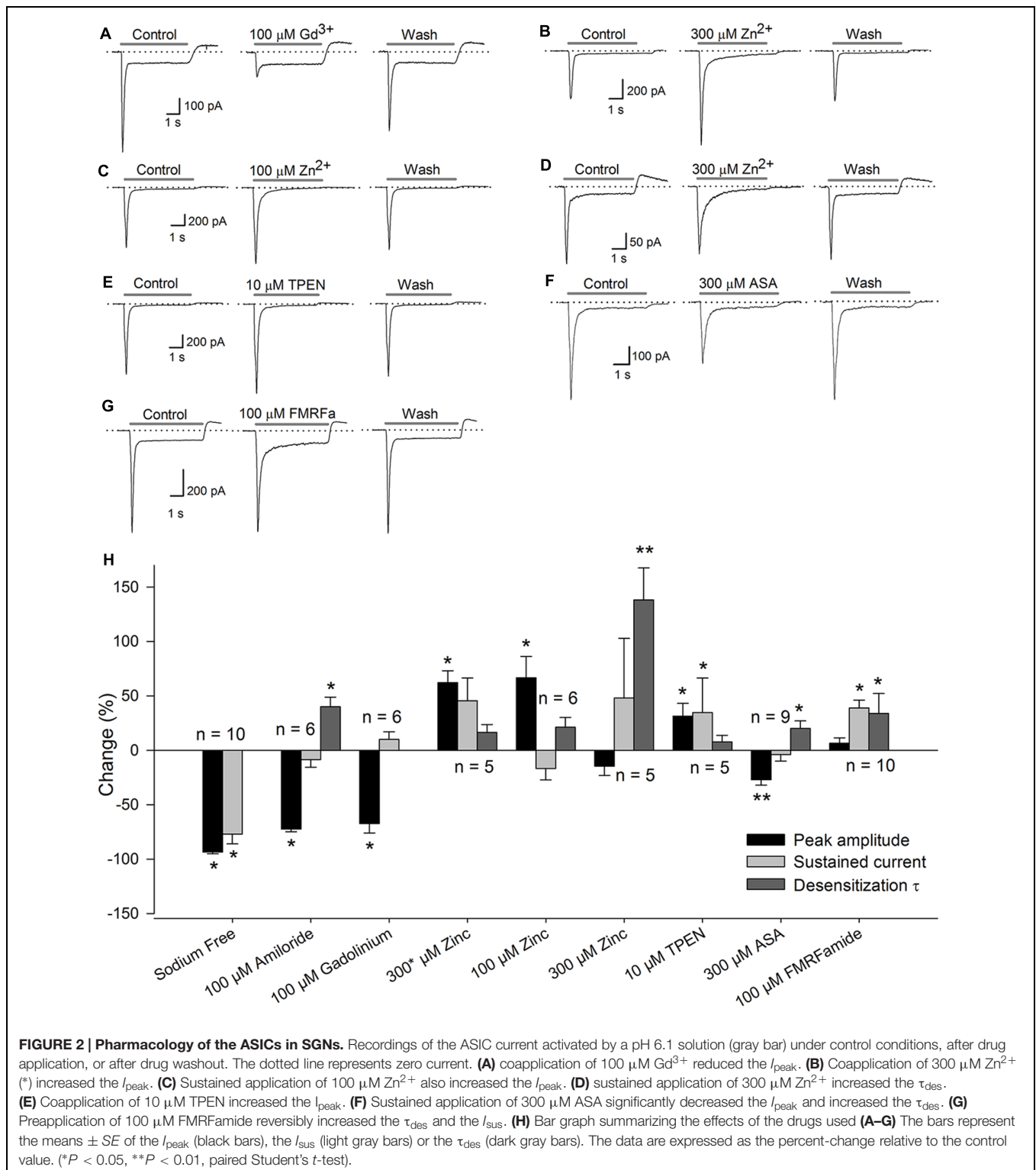
Effect of Aminoglycosides on the ASIC Current

Aminoglycosides are widely used antibiotics that exert well-known ototoxic effects. Garza et al. (2010) found that in DRG neurons (DRGn), St, Neo, and gentamycin decrease the I_{peak} of ASIC current and increase its τ_{des} and the I_{int} . In SGNs, $100 \mu M$ St ($n = 10$) and $100 \mu M$ Neo ($n = 6$) significantly decreased the peak of the ASIC current by 38 ± 5 and $26 \pm 5\%$, respectively ($P < 0.05$ for both), and increased the τ_{des} by 840 ± 170 and $137 \pm 44\%$, respectively ($P < 0.05$ for both)

(Figure 3). The I_{int} was increased by 46 ± 11 and $42 \pm 6\%$ due to St and Neo application, respectively ($P < 0.05$ for both). Neither aminoglycoside altered the I_{sus} . Applying $50 \mu M$ St ($n = 7$) decreased the I_{peak} by $33 \pm 4\%$ ($P < 0.05$), enhanced the I_{sus} by $34 \pm 13\%$ ($P < 0.05$), increased the I_{int} by $17 \pm 6\%$ ($P < 0.05$) and increased the τ_{des} by $132 \pm 33\%$ ($P < 0.05$). Applying $50 \mu M$ Neo ($n = 6$) decreased the I_{peak} by $11 \pm 3\%$ ($P < 0.05$), increased the τ_{des} by $107 \pm 26\%$ ($P < 0.05$), and increased the I_{int} by $28 \pm 10\%$ ($P < 0.05$) but did not significantly alter the I_{sus} (Figure 3C). The effects of St and Neo were dose-dependent (one-way ANOVA: $P < 0.05$). Increasing of τ_{des} causes an increase in the I_{int} , consequently increasing Na^+ entry, which most likely causes substantial depolarization and, therefore, hyperexcitation of SGNs, which may contribute to the ototoxic effects of aminoglycosides.

ASIC Current in the Onset of Hearing

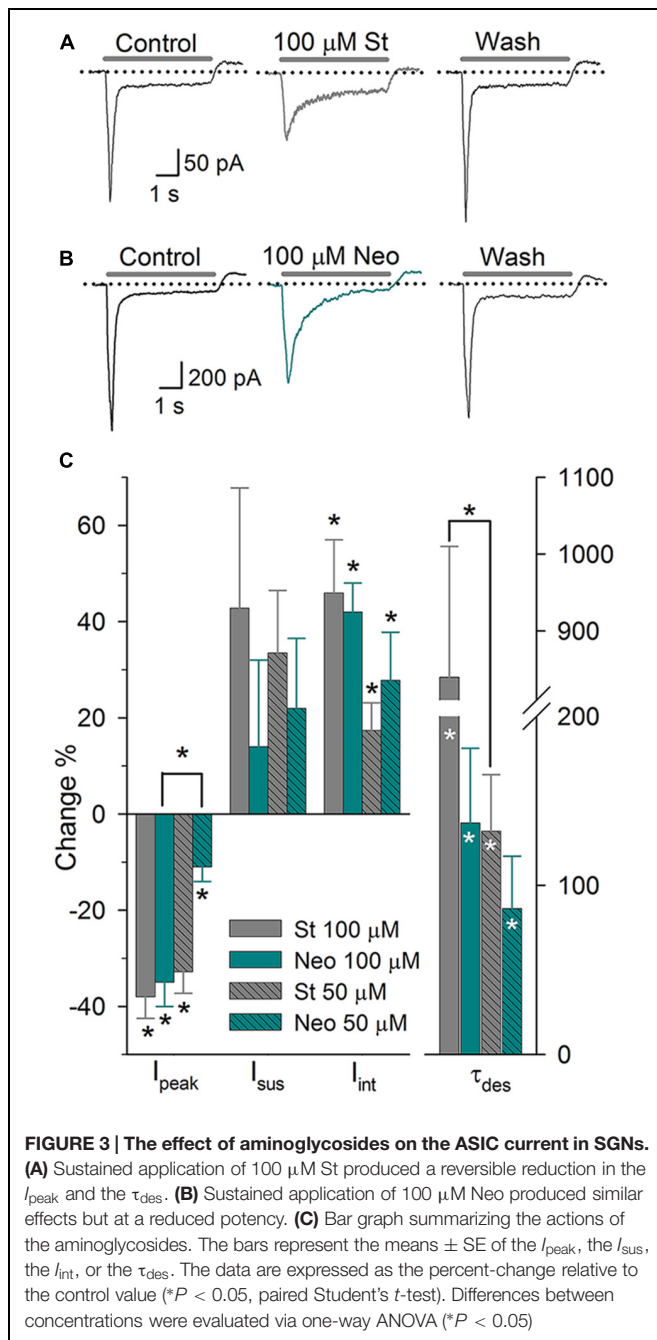
The onset of hearing is at P12 in mice. At this stage the IHC and afferent ends synapses are completely formed. Moreover, the activity of auditory nerve is mature between P12 and P20 (Shnerson and Pujol, 1981). In SGN cultured from P14–16 mice we also found electrophysiological and pharmacological evidence of functional ASIC currents. Amiloride ($100 \mu M$, $n = 11$) blocked I_{peak} $31 \pm 5\%$ ($P < 0.05$) and increased τ_{des} $170 \pm 40\%$ ($P < 0.05$) (Figure 4A). No effect on I_{sus} was observed. Second, FMRamide ($n = 12$, $100 \mu M$) increased the I_{peak} and I_{sus} as well as desensitization rate 27 ± 6 , 73 ± 15 , and $164 \pm 28\%$, respectively (Figure 4B). And finally, $100 \mu M$ St ($n = 5$) blocked the I_{peak} $38 \pm 5\%$, increased I_{sus} and desensitization rate 29 ± 9 and



670 \pm 170%, respectively (**Figures 4A,B**). These results showed ASIC channels to be functionally present in mature cochlea.

Some effects on P14–16 mice were different from those observed in P3–5 mice. In the case of amiloride, both effects were significantly different from each other (I_{peak} and desensitization

rate; ANOVA, $P < 0.01$). Besides, FMRFamide effects on the I_{peak} and I_{sus} were significantly different between these two stages (ANOVA, $P < 0.01$). All the effects observed in St treatment were not different between the two groups of mice.



ASIC Subunit Expression

RT-PCR was performed on the cDNA obtained from the SG to examine the ASIC subunits expression in the SGN. The brain (B) was used as positive control. The predicted sizes of the four *Asic* gene-related PCR fragments were detected in both the SG and the B (Figures 5A,B). mRNA corresponding to the 18S ribosomal subunit was used as constitutive expression control gene (Figure 5C). Relative to B *Asic* subunit expression levels were calculated using the $2^{-\Delta\Delta C_t}$ method (Livak and Schmittgen, 2001). The expression levels of *Asic1*, *Asic2*, and *Asic4* were lower in the SG than in the B. By contrast, the

Asic3 expression level was considerably higher, by approximately 30-fold, in the SG than in the B (Figure 5D). This result is in agreement with previous results comparing *Asic3* expression between the brain and the cochlea (Hildebrand et al., 2004).

The high intensity of *Asic2* band in SGNs suggests a high expression level; however, this implication is not conclusive because this method does not involve absolute quantification. The absence of genomic DNA from our RNA samples was confirmed based on negative controls in which reverse transcription was omitted (Figure 5). The expression of the four ASIC subunits demonstrated via RT-PCR is in agreement with the electrophysiological and pharmacological results.

Immunohistochemical Localization of ASIC Channels in SG

The localization of ASIC subunit IR in the mouse cochlea was examined by immunofluorescence and immunoperoxidase staining.

Based on immunofluorescence, the four ASIC subunits (ASIC1, 2, 3, and 4) were detected in SG (Figures 6A–E). ASIC3 and ASIC2 displayed the highest level of staining in SGNs. All of the ASICs displayed uniform staining of the SGNs. Immunostaining of primary cultured neurons (Figures 6F–J) demonstrated the presence of the ASIC1, 2, 3, and 4 subunits; the corresponding antibodies uniformly stained the cell bodies.

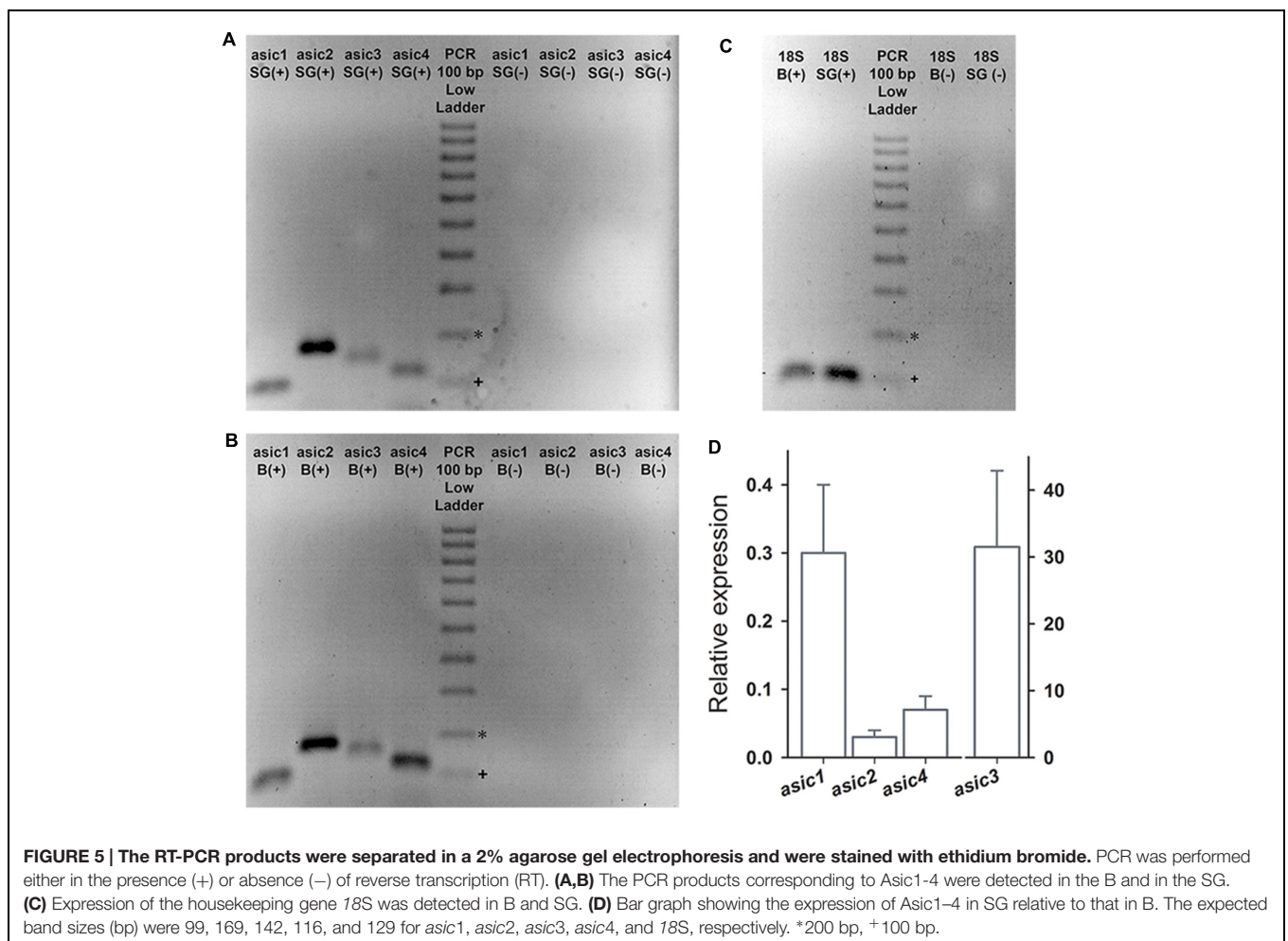
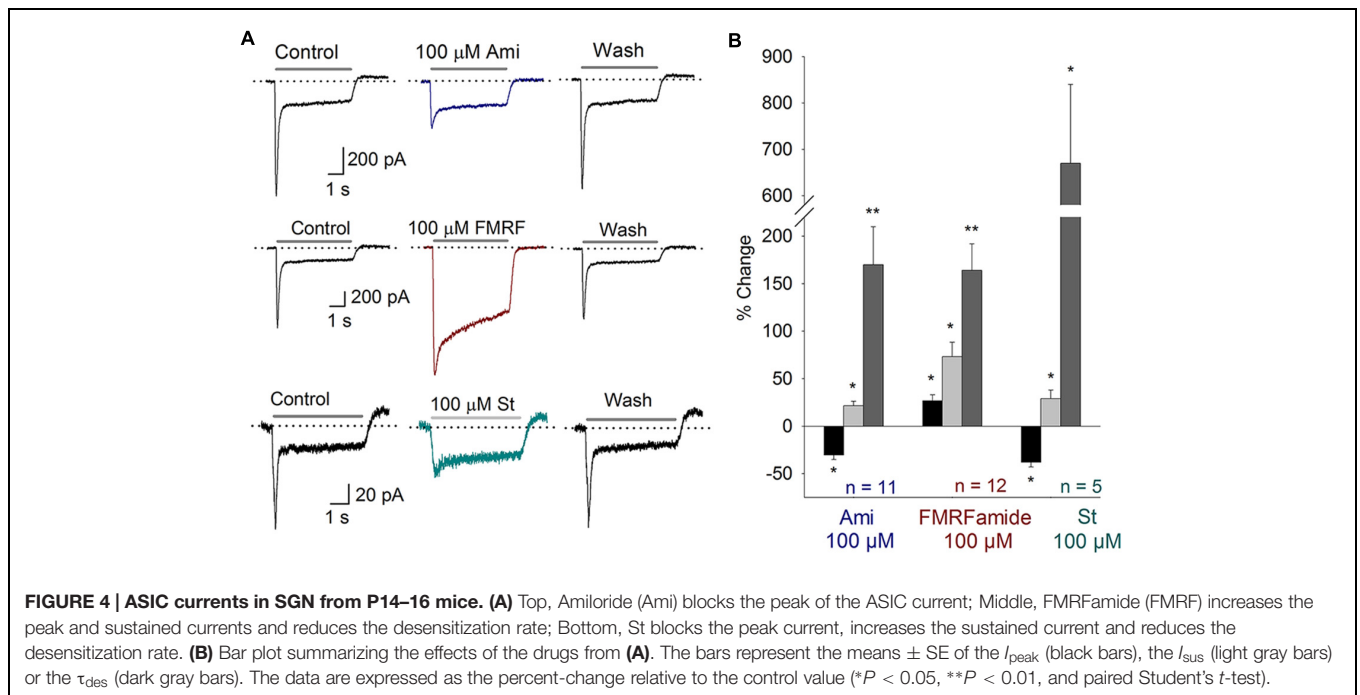
An additional experiment (ADI series) using antibodies from a different source was performed to confirm the expression of ASIC subunits in SG and to determine the IR of the ASIC1 and ASIC2 splice variants (ASIC1a, ASIC1b, ASIC2a, and ASIC2b). ASIC2a and ASIC2b were detected in mouse SGNs via immunofluorescence (Figures 6K–N). This result is in agreement with previous results in which ASIC2a and 3 were detected in the mouse cochlea (Hildebrand et al., 2004; Peng et al., 2004).

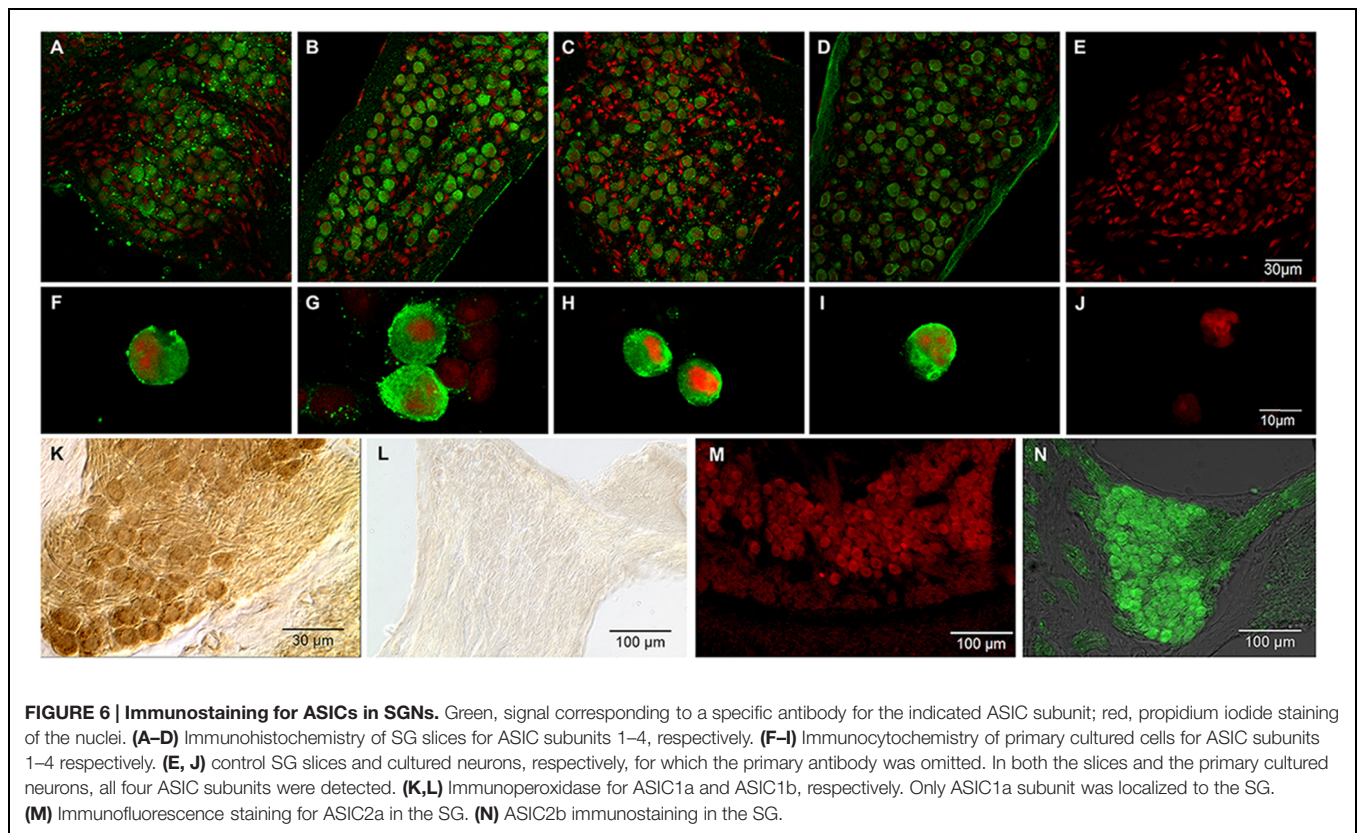
The IR of ASIC1a and ASIC1b were examined using immunoperoxidase staining. The ASIC1a subunit was detected in the SG. Interestingly, ASIC1b was not detected in the SG (Figures 6K,L).

Other cochlear structures, such as the tectorial membrane and the stria vascularis, were also stained by the ASIC1, 2 and 4 antibodies. Slices of the whole cochlea showed ASIC1 immunostaining in the fibers running from spiral ganglion to the OC, and a faint staining at the hair cell base region, most likely due to the presence of afferent terminals (Figure 7).

ASIC Activity in Current-Clamp Experiments

Acidic extracellular solutions of pH 7.0, 6.1, 5.0, 4.5, and 4.0 were used to determine whether APs were generated by extracellular acidification. A total of 40 neurons were recorded, from physiological pH (7.4) and using acidic solutions (pH 6.1 and 4.5) 15% of the neurons fired an AP in response to the acidic pH perfusion (Figure 8A); the remaining neurons displayed a sustained pH-dependent depolarization, although the depolarization was above threshold for current discharge (more than 30 mV in some cells), the depolarization rising phase was relatively slow and no AP discharge was induced (Figure 8B).





The steady state desensitization curve (Figure 1A) indicated that at pH 7.8, there was maximal channel availability and, thus, maximal amplitude of the ASIC current. Therefore, we decided to perform experiments in which cells were bathed in preconditioning extracellular solution of pH 7.8. Under this condition, the pH 6.1 solution induced higher AP firing probability not shown.

To further elucidate the role of ASIC channels in SGN function, square, and sinusoidal currents were injected to induce AP discharges. Square pulses typically produced a single AP discharge and no further spiking, independently of the amplitude of the current used. Response was not modified by acidic solution perfusion although the acidic solutions added a significant depolarization of more than 10 mV. Altering the pH during the injection of sinusoidal current (10–40 Hz) depolarized the cell membrane and decreased the frequency and the amplitude of the APs in those cells stimulated with suprathreshold current injection that generated one AP phase locked in every cycle ($n = 30$). These results revealed a pH dependency of the ASIC current; at a more acidic pH, the depolarization of the SGNs was greater and longer, producing a greater inhibition of the AP discharges (Figure 9A). In all those cells stimulated with subthreshold sinusoidal current ($n = 13$) the acid solution perfusion produced APs in the rising phase of the depolarization, that were followed in some cells by no AP discharge during acid pulse perfusion (Figure 9B, $n = 8/13$) or by brief depolarization inhibition of the AP followed by a

transient or sustained discharge during the whole acid solution perfusion (Figure 9C).

Is the K_{Na} Activated by ASIC-mediated Na^+ Influx?

In 20% of the ASIC current recordings, an outward current component was detected after the acidic pulse. We hypothesized that this outward current may be the K_{Na} (Cervantes et al., 2013) that is activated by the Na^+ influx produced by the ASIC current. To test this hypothesis, extracellular Na^+ was replaced with Li^+ (pH 7.4 and 6.1). Sustained Li^+ perfusion resulted in an increase of the peak of the acid-gated current by $42 \pm 23\%$ ($P < 0.05$), a decrease in the I_{sus} by $35 \pm 9\%$ ($P < 0.01$), and a decrease in the post-ASIC activation outward current by $50 \pm 3\%$ ($P < 0.01$, $n = 7$), no change in the τ_{des} was detected (Figure 10). This result suggested that, in fact, the Na^+ influx through ASICs may activate the K_{Na} current, thus producing an outward current at the end of the acid-gated current. These results suggest that complex interactions between ASIC-mediated currents and other ionic currents may occur in SGNs.

DISCUSSION

The H^+ -gated current in mouse SGNs displayed rapid activation, partial desensitization that followed an exponential time course, and a sigmoidal sensitivity to the H^+ concentration, with a pH_{50} of 6.2. Steady-state desensitization was fitted to a sigmoidal curve

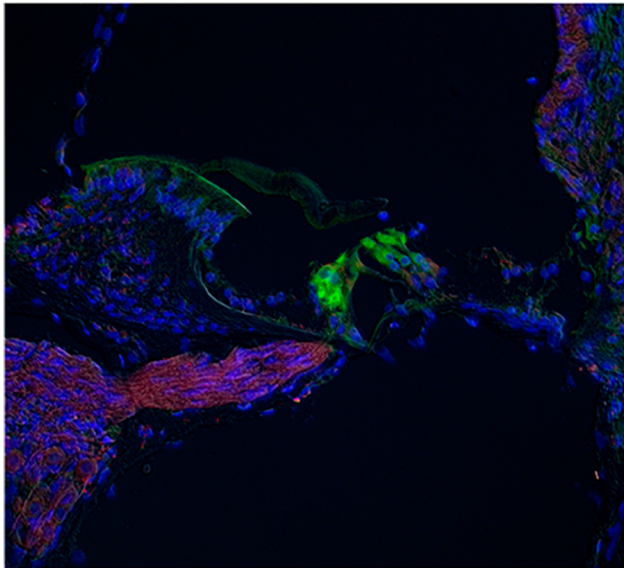


FIGURE 7 | Immunostaining for ASIC1 in whole cochlea slices. The IR for ASIC1 (red) was found in the fibers running from spiral ganglion to the OC, and a faint staining at the hair cell base region, most likely due to the presence of afferent terminals. The IR to calmodulin (green) was located at the hair cells. Blue staining corresponds to nuclei stained with DAPI.

with a pH_{50} of 7.3. The activation and steady-state desensitization curves displayed a window current in which a significantly high open probability was detected at pH 6.5–8.0. The proton-gated current was carried by Na^+ ; reduced by amiloride, Gd^{3+} , low concentrations (nM) of Zn^{2+} , and ASA; and enhanced by FMRamide and high concentrations (μM) of Zn^{2+} . We

found that all four ASIC mRNAs are expressed in SGNs and the ASIC-1a, -2a, -2b, -3, and -4 proteins are detectable via immunohistochemistry.

Pharmacological analysis revealed that the ASIC1, ASIC2a, and ASIC3 subunits are functionally expressed in SGNs. No drugs acting upon the ASIC1b, 2b, and 4 subunits have been described; thus, no pharmacological evidence for their functional expression was obtained. Regarding the action of Gd^{3+} , this ion typically inhibits ASIC3 homomeric and ASIC2a+3 heteromeric channels (Babinski et al., 2000) indicating the functional participation of these two subunits (ASIC2a and 3) in SGNs. FMRamide peptide has been shown to produce a slowing of the current desensitization and to increase the I_{sus} in ASIC channels conformed by ASIC1 and 3 subunits (Askwith et al., 2000). In this study, FMRamide potentiated the ASIC currents suggesting the functional presence of the ASIC1 and ASIC3 subunits in the SGN. Previous reports have indicated that Zn^{2+} binds to ASIC to a low-affinity site in the extracellular loop of the ASIC2a subunit (His 62 and 339), potentiating the ASIC current (Baron et al., 2001). We found that coapplication of Zn^{2+} in the μM range resulted in an increment of the current amplitude, indicating that ASIC2a is incorporated into SGN ASICs. It has also been shown that sustained perfusion of Zn^{2+} in the μM range inhibits ASIC3 homomeric and heteromeric ASICs (Jiang et al., 2010). In SGNs, sustained application of Zn^{2+} in the μM range increased the τ_{des} but did not affect the I_{peak} . Zn^{2+} also binds to a high-affinity site on ASIC1a (Lys-133) that may constitutively inhibit the activity of ASIC1a homomers and ASIC1a–2a heteromers (Chu et al., 2004), as most of the salts used to prepare physiological solutions in laboratories contain trace amounts of Zn^{2+} (approximately 20–50 nM; Paoletti et al., 1997). Applying a Zn^{2+} chelator (TPEN) in our experiments produced a significant increase

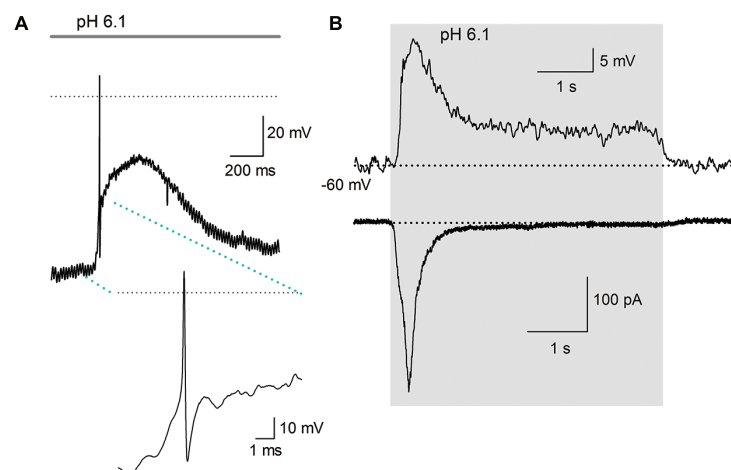
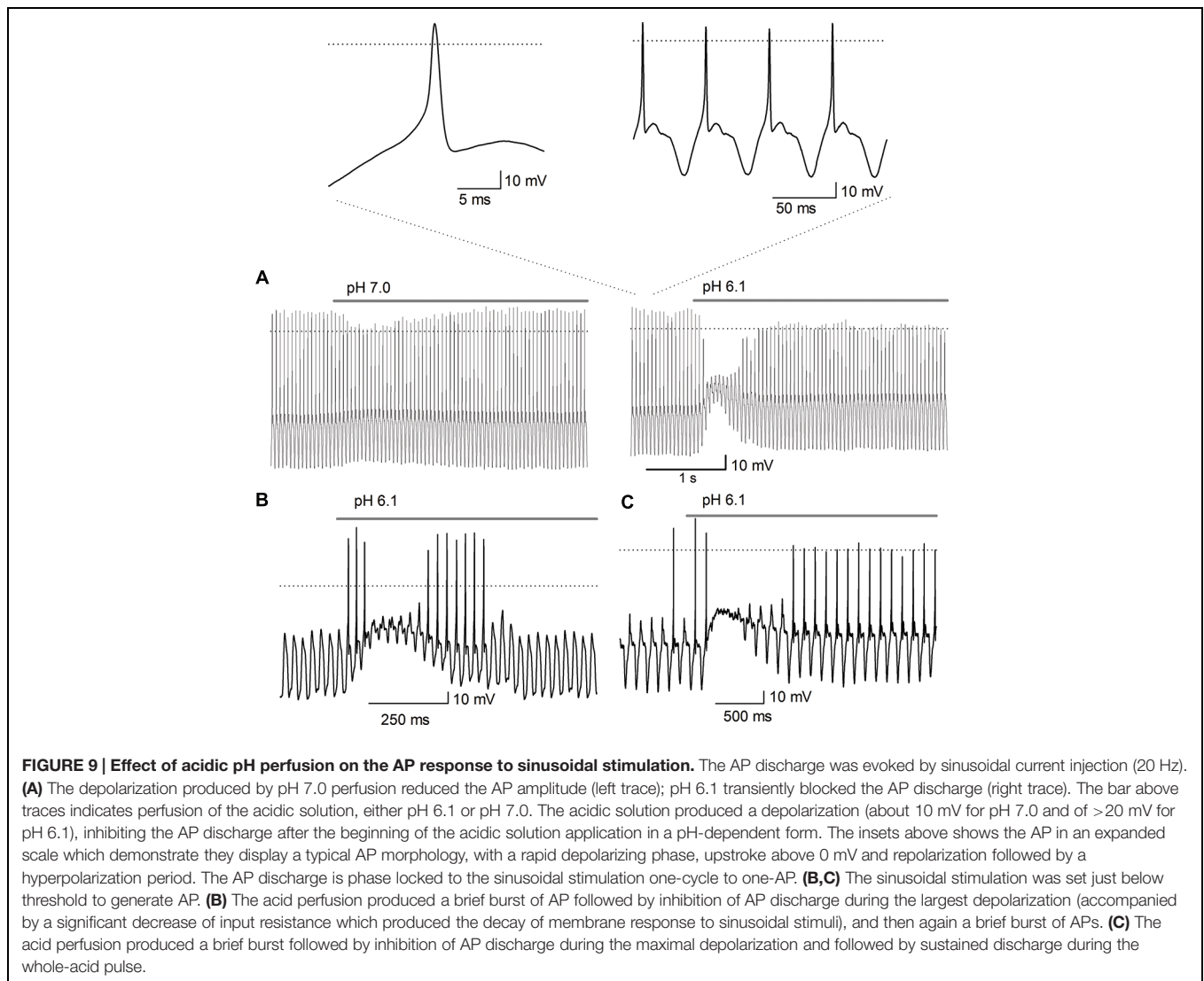


FIGURE 8 | Action potential discharges are activated by acidic solution. (A) An AP evoked in response to a pH 6.1 solution; inset shows the AP in larger scale. Only one AP discharge occurred, followed by a large depolarization of about 40 mV. The dotted line represents zero voltage, and line at the top indicates the duration of acidic extracellular perfusion. The membrane potential was set at about -90 mV. **(B)** Current and voltage clamp recording from a cell. Above the current clamp recording shows that acid perfusion (from pH 7.4–6.1 -grey area), evoked no AP discharge although a slowly raising depolarization of >20 mV was induced in response to a pH 6.1 solution perfusion. The time course of the depolarization and its decay neatly follows the time course of the inward current (below) caused by the acidic solution. The dotted line indicates -60 mV for current clamp and 0 pA for voltage clamp recording.



in the ASIC I_{peak} , indicating the participation of the ASIC1a subunit.

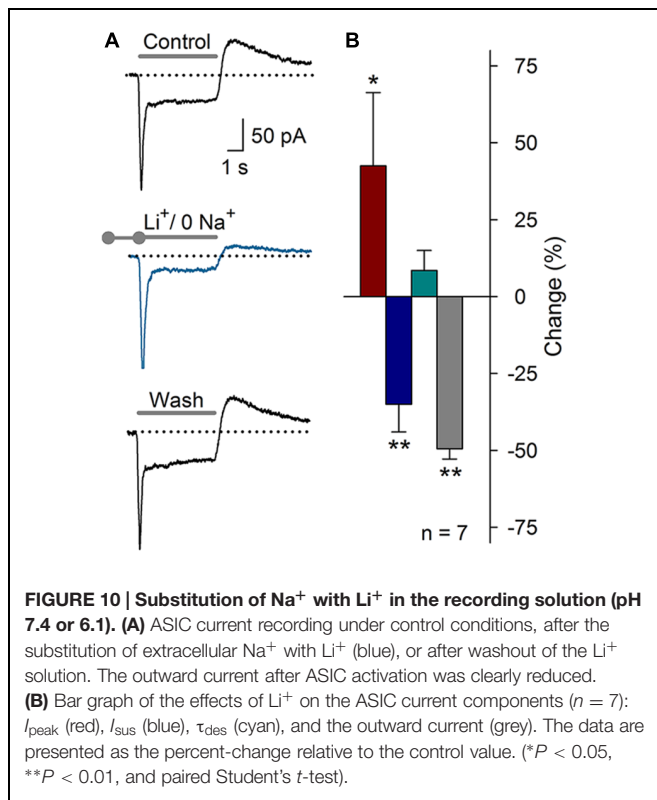
The Zn^{2+} -mediated modulation of the ASIC current in SGNs is complex because the ASICs in these neurons are most likely heteromeric. Nanomolar Zn^{2+} concentrations inhibit ASIC1a homomers or heteromers, and micromolar Zn^{2+} concentrations stimulate ASIC2a and ASIC3 homo or heteromers, making it difficult to predict the ultimate effect of Zn^{2+} on these channels. Nevertheless, we identified three possible effects of Zn^{2+} , supporting the concept that ASIC1a, 2a, and 3 are functionally expressed in SGNs.

According to our RT-PCR and immunohistochemistry results, all four ASIC subunits are expressed in the SGN. Although no information about their assembly was obtained, these ASICs are most likely assembled as heteromers, which may account for the diversity of the pharmacological effects that we observed. These results coincide with reports showing that when the same cell expresses different ASIC subunits, the assembled ASIC tend to include all of the expressed subunits (Benson et al., 2002;

Hesselager et al., 2004). The expression level of ASICs based on RT-PCR was expected because the *Asic3* subunit has been shown to be expressed in the PNS (Waldmann et al., 1997b). The higher expression level of *Asic3* in the SGNs than in the B is in agreement with a previous study of SGNs (Hildebrand et al., 2004).

The expression and distribution of ASICs based on immunohistochemistry strongly agree with our physiological and pharmacological results, and coincided with previous studies, in which ASIC2a and 3 were detected in SGNs (Hildebrand et al., 2004; Peng et al., 2004). Moreover, electrophysiology and pharmacological evidences demonstrate that ASIC current is still functional in mice after the onset of hearing. Amiloride and FMRFamide effects in P14–15 mice were more potent. These data suggest a change in ASIC subunit expression in SGN after the onset of hearing.

The aminoglycoside antibiotics increased the τ_{des} , and the I_{sus} of ASIC currents of DRG neurons (Garza et al., 2010) resulting in a higher Na^+ entry and probably Ca^{2+} entry. These findings were particularly interesting because clinical use



of aminoglycoside antibiotics is a major cause of non-genetic hearing loss; mechanisms include hair cell death following intracellular accumulation. These molecules also act directly on ASIC currents in SGN increasing the τ_{des} , and the *I*_{sus}, this could be a possible mechanism contributing to their ototoxic effect by increasing Na⁺ and Ca²⁺ entry through ASIC channels.

A slowly activating outward after-current was detected following ASIC current activation in 20% of the cells. Activating ASIC channels produces an increase in intracellular Na⁺ concentration, which could activate *K*_{Na} channels to generate an outward after-current. Interestingly, *K*_{Na} channels are not activated by Li⁺ (Bhattacharjee and Kaczmarek, 2005; Cervantes et al., 2013), whereas ASIC channels are highly permeable to this ion (Waldmann et al., 1997a). The use of Li⁺ instead of Na⁺ as an ASIC current carrier significantly decreased the outward after-current, indicating that *K*_{Na} channels activation in SGNs could be coupled to ASIC channels activation.

In current-clamp experiments extracellular acidification induced a significant depolarization of the SGNs and AP discharge in 15% of them. SGN were held at -60 and -90 mV, the most hyperpolarizing voltage was used to increase sodium voltage-gated channel availability. However, no differences were found between these two membrane potentials. Apparently, AP discharge is most likely due to ASIC channels availability, which is less than 40% at pH 7.4 as showed in the desensitization curve (Figure 1A). Increasing ASIC channel availability using pH 7.8 extracellular solution resulted in a higher AP firing probability. Thus, ASIC channel availability is playing a role in the SGN excitability, and not only acidification but alkalization of the

media may produce a significant effect in the ASIC current functional role. Failure to evoke AP firing in some cells could be due to the slow rise time of depolarization induced by the ASIC current, giving time to sodium voltage-gated channels to inactivate (Santos-Sacchi, 1993). Also the inhibition of the Na⁺ current may account for the AP inhibition during acid solution perfusion; in fact the decrease of the AP amplitude indicate that this is taken place in our system (Hille, 1971).

In vivo, SGNs basally discharge in response to ongoing synaptic transmission from the cochlear hair cells. To look for modulatory actions of pH on the afferent activity, AP discharge was evoked with sinusoidal current injection and SGN activity modulation by extracellular protons showed that increased acidity depolarized the membrane and reduced the ongoing AP activity. These results are analogous to those in hippocampal neurons, where ASIC activation terminated the AP burst in a pH-dependent manner (Vukicevic and Kellenberger, 2004). However, in most of the cells stimulated with subthreshold sinusoidal current injection, the acid perfusion induced APs discharge during the rising phase of the depolarization and in about 10% of the cells there were a sustained discharge during the whole-acid perfusion (5 s), demonstrating that ASIC activation produces a significant excitatory input to the cochlear afferent neurons.

The ASICs are located in postsynaptic regions (Wemmie et al., 2003, 2008; Ettaiche et al., 2004, 2006). Furthermore, rapid, transient synaptic cleft acidification due to the acid content (pH 5.7) of synaptic vesicles has been observed (Krishtal et al., 1987; Miesenböck et al., 1998; Du et al., 2014). Moreover, in CNS it has been shown that protons and ASIC channels are required for synaptic plasticity (Du et al., 2014; Kreple et al., 2014). Additionally, in the vestibular system a non-quantal excitatory postsynaptic current was caused by cleft acidification (Highstein et al., 2014). Otherwise, there is evidence that protons modulate synaptic transmission and afferent neurons excitability in mammalian vestibular system via ASIC channels (Mercado et al., 2006, 2012; Almanza et al., 2008). In SGN the ASIC channels may be activated by mechanically evoked proton release from hair cells, either via vesicular release of protons along with glutamate (intravesicular pH is 5.7) or by other mechanisms such as Na⁺/H⁺ exchange or electrogenic Na⁺/HCO₃ cotransport (Diering and Numata, 2014). This is the first report involving all ASIC subunits contributing to the SGN proton gated current covering functional, expression and immunolocalization. The evidence presented shows that protons have a modulatory role in cochlear afferent neurons excitability by acting on ASIC channels and promoting their depolarization.

AUTHOR CONTRIBUTIONS

ES and RV designed the project and participated in all aspects of the experimental work. AG-G was a doctoral student and realized the most part of the experiments. FM was postdoctoral researcher who realized part of the PCR and immunohistochemistry experiments. IL contributed with part of

the immunohistochemistry experiments. ES, RV, and AG-G written the first draft of the manuscript and all authors contributed to refine and finish the English text of the manuscript.

ACKNOWLEDGMENTS

This study was supported by grant from Consejo Nacional de Ciencia y Tecnología de México (CONACyT, grant

167052 to ES), and by grants from Vicerrectoria de Investigación y Estudios de Posgrado (VIEP-BUAP grants to RV and ES), and by grant CA Neurociencias 229866 and PROFOCIE 2014. AG-G was supported by CONACyT fellowship 206623. The Authors appreciate the support from Laboratorio Nacional de Microscopia Avanzada (LNMA) of the Biotechnology Institute of Universidad Nacional Autónoma de México (UNAM). Editing of the English manuscript was performed by Nature Publishing Group Language Editing.

REFERENCES

- Almanza, A., Mercado, F., Vega, R., and Soto, E. (2008). Extracellular pH modulates the voltage-dependent Ca^{2+} current and low threshold K^{+} current in hair cells. *Neurochem. Res.* 33, 1435–1441. doi: 10.1007/s11064-007-9565-9
- Askwith, C. C., Cheng, C., Ikuma, M., Benson, C., Price, M. P., and Welsh, M. J. (2000). Neuropeptide FF and FMRFamide potentiate acid-evoked currents from sensory neurons and proton-gated DEG/ENaC channels. *Neuron* 2, 133–141. doi: 10.1016/S0896-6273(00)81144-7
- Babinski, K., Catarsi, S., Biagini, G., and Seguela, P. (2000). Mammalian ASIC2a and ASIC3 subunits co-assemble into heteromeric proton-gated channels sensitive to Gd^{3+} . *J. Biol. Chem.* 275, 28519–28525. doi: 10.1074/jbc.M004114200
- Baron, A., Schaefer, L., Lingueglia, E., Champigny, G., and Lazdunski, M. (2001). Zn^{2+} and H^{+} are coactivators of acid-sensing ion channels. *J. Biol. Chem.* 276, 35361–35367. doi: 10.1074/jbc.M105208200
- Benson, C. J., Xie, J., Wemmie, J. A., Price, M. P., Henss, J. M., Welsh, M. J., et al. (2002). Heteromultimers of DEG/ENaC subunits form H^{+} -gated channels in mouse sensory neurons. *Proc. Natl. Acad. Sci. U.S.A.* 99, 2338–2343. doi: 10.1073/pnas.032678399
- Bhattacharjee, A., and Kaczmarek, L. K. (2005). For K^{+} channels, Na^{+} is the new Ca^{2+} . *Trends Neurosci.* 28, 422–428. doi: 10.1016/j.tins.2005.06.003
- Cervantes, B., Vega, R., Limon, A., and Soto, E. (2013). Identity, expression and functional role of the sodium-activated potassium current in vestibular ganglion afferent neurons. *Neuroscience* 240, 163–175. doi: 10.1016/j.neuroscience.2013.02.052
- Chu, X. P., Wemmie, J. A., Wang, W. Z., Zhu, X. M., Saugstad, J. A., Price, M. P., et al. (2004). Subunit-dependent high affinity zinc inhibition of acid-sensing ion channels. *J. Neurosci.* 24, 8678–8689. doi: 10.1523/JNEUROSCI.2844-04.2004
- Deval, E., Noël, J., Lay, N., Alloui, A., Diochot, S., Friend, V., et al. (2008). ASIC3, a sensor of acidic and primary inflammatory pain. *EMBO J.* 27, 3047–3055. doi: 10.1038/emboj.2008.213
- Diering, G. H., and Numata, M. (2014). Endosomal pH in neuronal signaling and synaptic transmission: role of $\text{Na}^{+}/\text{H}^{+}$ exchanger NHE5. *Front. Physiol.* 4:412. doi: 10.3389/fphys.2013.00412
- Du, J., Reznikov, L. R., Price, M. P., Zha, X. M., Lu, Y., Moninger, T. O., et al. (2014). Protons are a neurotransmitter that regulates synaptic plasticity in the lateral amygdala. *Proc. Natl. Acad. Sci. U.S.A.* 111, 8961–8966. doi: 10.1073/pnas.1407018111
- Ettaiche, M., Deval, E., Cougnon, M., Lazdunski, M., and Voilley, N. (2006). Silencing Acid-Sensing Ion Channel 1a alters cone-mediated retinal function. *J. Neurosci.* 26, 5800–5809. doi: 10.1523/JNEUROSCI.0344-06.2006
- Ettaiche, M., Guy, N., Hofman, P., Lazdunski, M., and Waldmann, R. (2004). Acid-sensing ion channel 2 is important for retinal function and protects against light-induced retinal degeneration. *J. Neurosci.* 24, 1005–1012. doi: 10.1523/JNEUROSCI.4698-03.2004
- Friese, M. A., Craner, M. J., Eitzenperger, R., Vergo, S., Wemmie, J. A., Welsh, M. J., et al. (2007). Acid-sensing ion channel-1 contributes to axonal degeneration in autoimmune inflammation of the central nervous system. *Nat. Med.* 13, 1483–1489. doi: 10.1038/nm1668
- Garza, A., López-Ramírez, O., Vega, R., and Soto, E. (2010). The aminoglycosides modulate the acid-sensing ionic-channel (ASIC) currents in dorsal-root ganglion neurons from the rat. *J. Pharmacol. Exp. Ther.* 332, 489–499. doi: 10.1124/jpet.109.152884
- Goutman, J. D., and Glowatzki, E. (2007). Time course and calcium dependence of transmitter release at a single ribbon synapse. *Proc. Natl. Acad. Sci. U.S.A.* 104, 16341–16346. doi: 10.1073/pnas.0705756104
- Hesselager, M., Timmermann, D. B., and Ahning, P. K. (2004). pH Dependency and desensitization kinetics of heterologously expressed combinations of acid-sensing ion channel subunits. *J. Biol. Chem.* 279, 11006–11015. doi: 10.1074/jbc.M313507200
- Highstein, S. M., Holstein, G. R., Mann, M. A., and Rabbitt, R. D. (2014). Evidence that protons act as neurotransmitters at vestibular hair cell-calyx afferent synapses. *Proc. Natl. Acad. Sci. U.S.A.* 111, 5421–5426. doi: 10.1073/pnas.1319561111
- Hildebrand, M. S., de Silva, M. G., Klockars, T., Rose, E., Price, M., Smith, R. J., et al. (2004). Characterization of DRASIC in the mouse inner ear. *Hear. Res.* 190, 149–160. doi: 10.1016/S0378-5955(04)00015-2
- Hille, B. (1971). The permeability of the sodium channel to organic cations in myelinated nerve. *J. Gen. Physiol.* 58, 599–619. doi: 10.1085/jgp.58.6.599
- Jiang, Q., Papsian, C. J., Wang, J. Q., Xiong, G., and Chu, X. P. (2010). Inhibitory regulation of acid-sensing ion channel 3 by zinc. *J. Neurosci.* 169, 574–583. doi: 10.1016/j.neuroscience.2010.05.043
- Kreple, C. J., Lu, Y., Taugher, R. J., Schwager-Gutman, A. L., Du, J., Stump, M., et al. (2014). Acid-sensing ion channels contribute to synaptic transmission and inhibit cocaine-evoked plasticity. *Nat. Neurosci.* 17, 1083–1091. doi: 10.1038/nn.3750
- Krishtal, O. A., Osipchuk, Y. V., Shelest, T. N., and Smirnov, S. V. (1987). Rapid extracellular pH transients related to synaptic transmission in rat hippocampal slices. *Brain Res.* 436, 352–356. doi: 10.1016/0006-8993(87)91678-7
- Livak, K. J., and Schmittgen, T. D. (2001). Analysis of relative gene expression data using Real-Time quantitative PCR and the $2^{-\Delta\Delta\text{Ct}}$ method. *Methods* 25, 402–408. doi: 10.1006/meth.2001.1262
- Mercado, F., López, I., Ortega, A., Almanza, A., Soto, E., and Vega, R. (2012). FMRFamide-related peptide expression in the vestibular-afferent neurons. *Neurosci. Lett.* 513, 12–16. doi: 10.1016/j.neulet.2012.01.074
- Mercado, F., Lopez, I. A., Acuna, D., Vega, R., and Soto, E. (2006). Acid-sensing ionic channels in the rat vestibular endorgans and ganglia. *J. Neurophysiol.* 96, 1615–1624. doi: 10.1152/jn.00378.2006
- Miesenböck, G., De Angelis, D. A., and Rothman, J. E. (1998). Visualizing secretion and synaptic transmission with pH-sensitive green fluorescent proteins. *Nature* 394, 192–195. doi: 10.1038/28190
- Paoletti, P., Ascher, P., and Neyton, J. (1997). High-affinity zinc inhibition of NMDA NR1-NR2A receptors. *J. Neurosci.* 17, 5711–5725.
- Peng, B. G., Ahmad, S., Chen, S., Chen, P., Price, M. P., and Lin, X. (2004). Acid-sensing ion channel 2 contributes a major component to acid-evoked excitatory responses in spiral ganglion neurons and plays a role in noise susceptibility of mice. *J. Neurosci.* 24, 10167–10175. doi: 10.1523/JNEUROSCI.3196-04.2004
- Santos-Sacchi, J. (1993). Voltage-dependent ionic conductances of type I spiral ganglion cells from the guinea pig inner ear. *J. Neurosci.* 13, 3599–3611.
- Sherwood, T. W., Lee, K. G., Gormley, M. G., and Askwith, C. C. (2011). Heteromeric ASIC channels composed of ASIC2b and ASIC1a display novel channel properties and contribute to acidosis-induced neuronal death. *J. Neurosci.* 31, 9723–9734. doi: 10.1523/JNEUROSCI.1665-11.2011

- Shnerson, A., and Pujol, R. (1981). Age-related changes in the C57BL/6J mouse cochlea. I. Physiological findings. *Dev. Brain Res.* 2, 65–75. doi: 10.1016/0165-3806(81)90059-6
- Ugawa, S., Inagaki, A., Yamamura, H., Ueda, T., Ishida, Y., Kajita, K., et al. (2006). Acid-sensing ion channel-1b in the stereocilia of mammalian cochlear hair cells. *Neuroreport* 17, 1235–1239. doi: 10.1097/01.wnr.0000233093.67289.66
- Valdés-Baizabal, C., Soto, E., and Vega, R. (2015). Dopaminergic modulation of the voltage-gated sodium current in the cochlear afferent neurons of the rat. *PLoS ONE* 10:e0120808. doi: 10.1371/journal.pone.0120808
- Vega, R., Rodríguez, U., and Soto, E. (2009). Acid-sensing ionic-channel functional expression in the vestibular endorgans. *Neurosci. Lett.* 463, 199–202. doi: 10.1016/j.neulet.2009.07.086
- Vukicevic, M., and Kellenberger, S. (2004). Modulatory effects of acid-sensing ion channels on action potential generation in hippocampal neurons. *Am. J. Physiol. Cell Physiol.* 287, C682–C690. doi: 10.1152/ajpcell.00127.2004
- Waldmann, R., Champigny, G., Bassilana, F., Heurteaux, C., and Lazdunski, M. (1997a). A proton-gated cation channel involved in acid-sensing. *Nature* 386, 173–177. doi: 10.1038/386173a0
- Waldmann, R., Bassilana, F., Weille, J., Champigny, G., Heurteaux, C., and Lazdunski, M. (1997b). Molecular cloning of a non-inactivating proton-gated Na⁺ channel specific for sensory neurons. *J. Biol. Chem.* 272, 20975–20978. doi: 10.1074/jbc.272.34.20975
- Wemmie, J. A., Askwith, C. C., Lamani, E., Cassell, M. D., Freeman, J. H. Jr., and Welsh, M. J. (2003). Regions with high synaptic density and contributes to fear conditioning. *J. Neurosci.* 23, 5496–5502.
- Wemmie, J. A., Chen, J., Askwith, C. C., Hruska-Hageman, A. M., Price, M. P., Nolan, B. C., et al. (2002). The acid-activated ion channel ASIC contributes to synaptic plasticity, learning, and memory. *Neuron* 34, 463–477. doi: 10.1016/S0896-6273(02)00661-X
- Wemmie, J. A., Zha, X. M., and Welsh, M. (2008). “Acid-sensing ion channels (ASICs) and pH in synapse physiology,” in *Structural and Functional Organization of the Synapse*, (New York, NY: Springer), 661–681.
- Yagi, J., Wenk, H. N., Naves, L. A., and McCleskey, E. W. (2006). Sustained currents through ASIC3 ion channels at the modest pH changes that occur during myocardial ischemia. *Circ. Res.* 9, 501–509. doi: 10.1161/01.RES.0000238388.79295.4c
- Ziemann, A. E., Schnizler, M. K., Albert, G. W., Severson, M. A., Howard, M. A. III, Welsh, M. J., et al. (2008). Seizure termination by acidosis depends on ASIC1a. *Nat. Neurosci.* 11, 816–822. doi: 10.1038/nn.2132

Conflict of Interest Statement: The authors declare that the research was conducted in the absence of any commercial or financial relationships that could be construed as a potential conflict of interest.

Copyright © 2015 González-Garrido, Vega, Mercado, López and Soto. This is an open-access article distributed under the terms of the Creative Commons Attribution License (CC BY). The use, distribution or reproduction in other forums is permitted, provided the original author(s) or licensor are credited and that the original publication in this journal is cited, in accordance with accepted academic practice. No use, distribution or reproduction is permitted which does not comply with these terms.